The combined effect of pore radius and protein dielectric coefficient on the selectivity of a calcium channel

Dezső Boda[1,2*], Mónika Valiskó[2], Bob Eisenberg[1], Wolfgang Nonner[3], Douglas Henderson[4], Dirk Gillespie[1]
[1]*Department of Molecular Biophysics and Physiology, Rush University Medical Center, Chicago, IL 60612*
[2]*Department of Physical Chemistry, University of Pannon, P. O. Box 158, H-8201 Veszprém, Hungary*
[3]*Department of Physiology and Biophysics, University of Miami School of Medicine, Miami, FL 33101 and*
[4]*Department of Chemistry and Biochemistry, Brigham Young University, Provo, UT 84602*
(Dated: August 28, 2006)

Calcium-selective ion channels often contain a selectivity filter made of similar amino acids, rich in carboxylates, although the Ca^{2+} affinities of these channels range from micromolar to millimolar. To understand the physical mechanism for this range of affinities, we use grand canonical Monte Carlo simulations to study the competition of Na^+ and Ca^{2+} in the selectivity filter of a reduced model of a Ca channel. We show that Ca^{2+} affinity is increased dramatically when both the volume and dielectric coefficient of the protein are reduced.

PACS numbers: 41.20.Cv, 77.22.Ej, 02.70.Uu

The physical mechanism by which genetic information controls the ion-binding properties of proteins is an important topic in molecular biophysics. Here, we show that the pores of Ca^{2+}-selective ion channels (Ca channels) can bind Ca^{2+} with a range of specificities set by two parameters (the radius of the pore and the dielectric coefficient of the protein) that characterize protein properties in our low-resolution model. This model can also describe Ca^{2+}-binding pockets in many proteins besides ion channels. We vary a structural parameter—the radius of the pore—to change the packing fraction of groups directly involved in coordinating Ca^{2+} ions. The packing fraction is a low resolution parameter because our model does not include any specification of the exact positions of these coordinating atoms (the oxygen atoms of the terminal carboxyl groups of glutamate or aspartate residues found in Ca^{2+}-specific domains [1, 2]). We also vary a physical parameter—the electrical polarizability of the protein material that is near the coordinating groups. Proteins can implement complex polarization properties by allowing different movements of their many kinds of electric charge—permanent and induced—in their backbone and in amino acid residues. We describe this polarization in the matter around the Ca^{2+}-coordinating groups using a dielectric coefficient. In genetic terms, our parameters constitute phenotypes that might result from a variety of genetically encoded, specific atomic structures of protein. Identifying such parameters is also a first step in engineering proteins.

Calcium ions enter the cytosol through Ca channels (e.g., the L-type and ryanodine receptor, RyR, Ca channels) and then activate the function of many proteins. In this way, Ca^{2+} transduces a signal from an extracellular receptor into intracellular protein function. The selectivity filters of Ca channels preferentially accumulate Ca^{2+} over monovalent cations even though the monovalent cations are present at much higher concentrations. For example, in single channel current/voltage experiments with 100-150 mM bath Na^+ concentration, a few μM Ca^{2+} blocks Na^+ current in the L-type Ca channel, while it takes 1000 times as much Ca^{2+} (in the millimolar range) to have the same effect in the RyR channel. The different selectivity behavior of these channels is an evolutionary result of their different physiological functions. Despite their different Ca^{2+} affinities, the L-type and RyR Ca channels have a common structural motif of four glutamate (Glu) or Aspartate (Asp) amino acids in their selectivity filters [1, 2]. Both Glu and Asp have negatively charged (i.e., acidic) carboxyl residues that make the selectivity filter a negatively-charged, carboxylate-rich site. Carboxylate-rich pockets are also present in

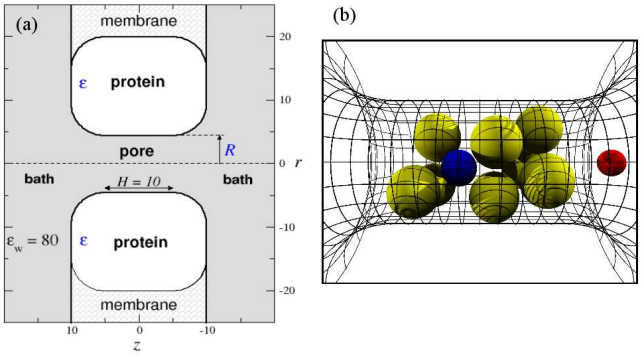

FIG. 1: (color online) (a) Geometry of the simulated Ca channel. This cross-section shows the central part of the cylindrical simulation cell (typically 75 Å in radius and 320 Å in length). (b) Snapshot from a simulation: ions in the pore (large yellow: $O^{1/2-}$; small blue in the center: Ca^{2+}; small red at the entrance: Na^+).

*Corresponding author, E-mail: dezso_boda@rush.edu

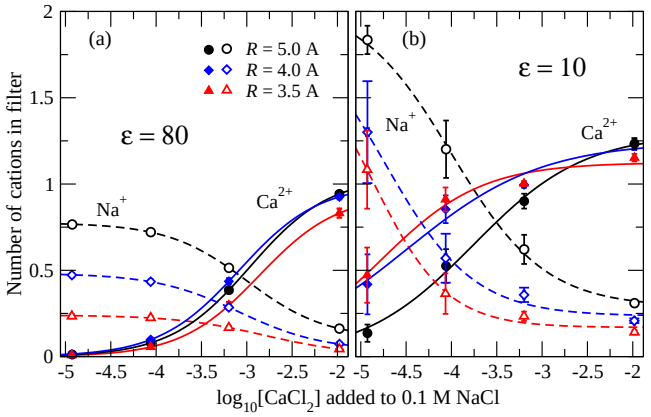

FIG. 2: (color online) The average numbers of Na^+ and Ca^{2+} ions in the cylindrical pore region (occupancy) vs. the logarithm of $CaCl_2$ concentration in the bath ([NaCl]=0.1 M). The symbols are simulation results; the curves are fitted using Eq. 7 of Ref. [8]; the fit includes a point obtained from a canonical MC simulation in the absence of $CaCl_2$ (not shown). Solid and dashed lines refer to Ca^{2+} and Na^+ ions, respectively.

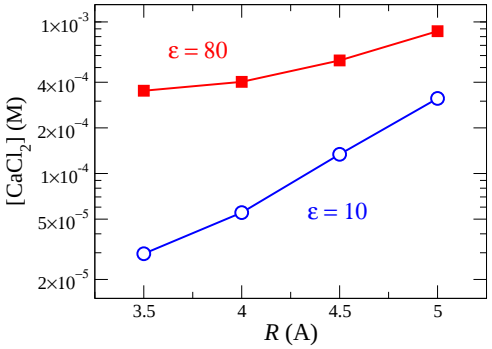

FIG. 3: (color online) The $[CaCl_2]$ where the occupancy curves for Ca^{2+} and Na^+ of Fig. 2 intersect, as a function of the radius of the pore.

many other proteins (e.g., proteins containing the EF-hand motif [3]), where they can bind Ca^{2+} with a wide range of affinities.

Ion conduction in L-type Ca channels has been modeled in molecular dynamics (MD) [4] and Brownian dynamics (BD) simulations [5]. The BD simutations suggested that the main driving force for divalent vs. monovalent selectivity is electrostatics [6], while other work has suggested that it is the balance of electrostatics with excluded volume in the crowded selectivity filter (the charge/space competition, CSC, model) [7, 8]. Both the MD and BD simulations were restricted to conditions of large ion concentrations and strong electric fields. In particular, the low Ca^{2+} concentrations of biological interest could not be modeled in these simulations. In previous work we have shown that Ca channels can be modeled in an appropriate ionic environment using Monte Carlo (MC) simulation and the grand canonical ensemble (GC) [9]. As far as we know, these are the first particle simulations of Ca^{2+}/protein interactions at the low Ca^{2+} concentrations at which they normally function. Here we use this technique to show that pore radius and dielectric environment together can tune Ca^{2+} affinity on a broad scale, from 1 mM (1000 μM) to 0.03 mM (30 μM), and that together the radius and dielectric coefficient produce a much larger effect than they do individually.

A cylindrical simulation cell is subdivided into two bath compartments by a membrane that contains a protein with a pore through it (Fig. 1a). These domains have hard boundaries that are impenetrable to ions. The protein (but not the pore) is assigned a dielectric coefficient that is either $\epsilon = 80$ (i. e., water-like) or $\epsilon = 10$. The dielectric coefficient in the rest of the cell (including the pore) is 80. A dielectric coefficient of 80 is used also for the membrane in order to reduce computation time for the electrostatics, but this does not affect the final results [9]. The electrolyte is represented in the primitive model, as hard-sphere ions with central charges. Ionic radii are 1, 0.99, and 1.81 Å for Na^+, Ca^{2+}, and Cl^-, respectively. The dimensions of the simulation cell are large enough to allow the formation of bulk-like solutions in both baths.

A snapshot from a MC simulation illustrates our reduced model of the central, cylindrical part of the pore that contains the charged COO^- groups of the protein's amino acids that extend into the ionic pathway (Fig. 1b). These COO^- groups are modeled here as distinct half charged oxygen ions ($O^{1/2-}$, radius 1.4 Å) that are restricted to the central cylinder of the pore so that they cannot overlap the cylinder boundaries. These oxygen particles act like free ions, except for their confinement. The radius of the confining central cylinder is varied between $R = 3.5$ and $R = 5$ Å, while the length of the cylinder is fixed at 10 Å.

We simulate a mixed thermodynamic ensemble where temperature (T=298.15 K), cell volume, and the number of Na^+ particles (300 in most runs) are fixed. The length and radius of the simulation cell are chosen so that the number of Na^+ yields a concentration of 0.1 M in the baths. Ca^{2+} and Cl^- particles are simulated in the GC ensemble by simultaneously inserting or deleting 1 Ca^{2+} and 2 Cl^- while maintaining a fixed chemical potential for $CaCl_2$. The Ca^{2+} concentrations in the baths are outputs of the simulations. The particle insertion/deletion step is coupled to a biased particle exchange between the channel and the bath to accelerate the convergence of the average number of Ca^{2+} and Na^+ ions in the channel [9, 10]. The electrostatic energy of the system is determined using the Induced Charge Computation (ICC) method [9, 11], which numerically solves an integral equation for the surface charge induced on dielectric boundaries. The ICC method gives accurate results even for curved boundaries.

For each ionic species, the affinity of the channel for

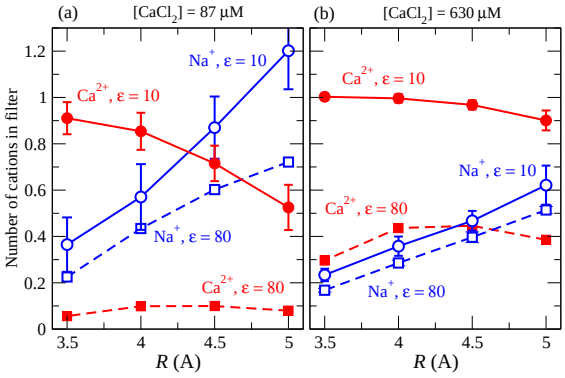

FIG. 4: (color online) The average number of Ca^{2+} and Na^{+} ions in the pore as a function of R for $\epsilon = 10$ and 80 at two fixed $[CaCl_2]$.

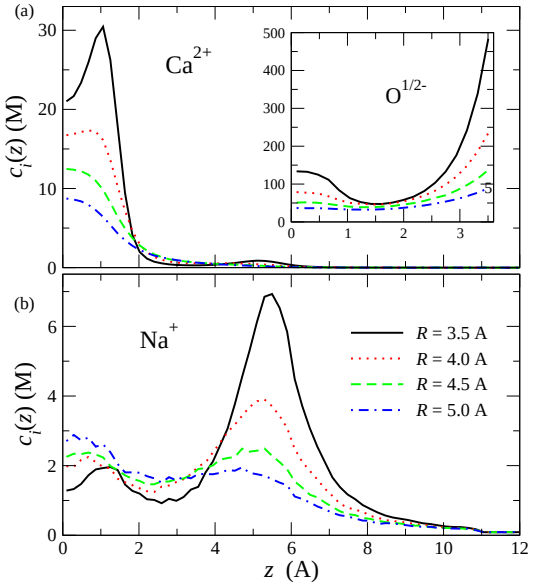

FIG. 5: (color online) Longitudinal profiles for (a) Ca^{2+} ($O^{1/2-}$, inset) and (b) Na^{+} ions in the pore for different pore radii, $\epsilon = 10$ and $[CaCl_2]$=630 μM. The concentration profiles are averages over the cross-section of the simulation cell.

that species is characterized by its occupancy, the average number of Ca^{2+} and Na^{+} ions located in the cylindrical pore ($|z| \leq 5$ Å). Ca^{2+} and Na^{+} occupancies are plotted as functions of $\log_{10}[CaCl_2]$ in the bath in Fig. 2. The figure shows that Ca^{2+} replaces Na^{+} in the filter as the bath Ca^{2+} concentration increases. We characterize the selectivity of the channel by the $[CaCl_2]$ at which the numbers of Ca^{2+} and Na^{+} in the filter are equal (i.e., the $[CaCl_2]$ where the Ca^{2+} and Na^{+} curves in Fig. 2 intersect). The smaller this $[CaCl_2]$, the more selective the channel is for Ca^{2+} over Na^{+}. We plot this characteristic concentration as a function of R in Fig. 3.

The figure shows that for a given radius Ca^{2+} vs. Na^{+} selectivity increases considerably when we reduce ϵ from 80 (squares) to 10 (circles). In the case of $\epsilon = 10$ more positive charge is attracted into the filter by the negative polarization charges induced by the oxygen ions on the wall of the pore (in the $\epsilon = 80$ case these induced charges are absent) [9]. This increased ionic density results in an increased hard sphere repulsion. The competition of these two effects results in a better Ca^{2+} vs. Na^{+} selectivity as ϵ decreases. Because of hard sphere exclusion, the pore is not electroneutral in our simulations; the structural charge of the pore is screened by counterions nearby in the vestibules and baths (see Fig. 6) rather than by counterions in the pore itself.

Figure 3 also shows that Ca^{2+} vs. Na^{+} selectivity increases only about 2-fold as the pore radius is reduced in the case of $\epsilon = 80$ (squares), while it increases much more (about 12-fold) in the case of $\epsilon = 10$ (circles). To gain an insight into this behavior, we consider the total numbers of Na^{+} and Ca^{2+} ions as functions of R for $[CaCl_2]$=87 and 630 μM in Fig. 4. In the case of $\epsilon = 80$, the number of Na^{+} in the pore becomes smaller as the size of the filter decreases, while the number of Ca^{2+} changes less (squares with dashed lines). For this reason, decreasing R increases Ca^{2+} vs. Na^{+} affinity, but only moderately. In the case of $\epsilon = 10$, the number of Na^{+} still decreases with decreasing R, but now the number of Ca^{2+} increases (circles with solid lines). As a consequence, better Ca^{2+} vs. Na^{+} selectivity is produced *both* by decreasing the amount of Na^{+} in the filter with decreasing R, *and* by increasing the number of Ca^{2+} (Fig. 5). Figure 5 also shows that the excluded Na^{+} ions accumulate at the entrances of the pore just outside the domain accessible to the oxygen ions where they contribute to the neutralization of the negative pore. This behavior becomes more pronounced at decreasing R.

To examine the interplay between excluded volume and electrostatics, we show the total number of cations N_{cation} (Fig. 6a) and the total number of cationic charges Q_{cation} (Fig. 6b) in the pore as functions of R. N_{cation} decreases with decreasing R (Fig. 6a) in every case because less space is available in the pore. Ionic densities become very high in the pore as R decreases (Fig. 5)and the CSC mechanism favors Ca^{2+} ions in the narrower channels (see Fig. 3) because Ca^{2+} provides twice the positive charge that Na^{+} does in the same ionic volume to balance the negative charges of the oxygens. In the case of $\epsilon = 80$, Q_{cation} decreases as R decreases because more counterions (primarily Na^{+}) are squeezed out of the pore. The electrostatic attraction provided by the oxygen ions is not enough to balance the increasing hard sphere exclusion.

In the case of $\epsilon = 10$, the net cationic charge Q_{cation} is quite unaffected as R decreases (Fig. 6b). Apparently, the electrostatics of the pore embedded in the weak dielectric is strong enough to keep *countercharge* in the pore even as the pore radius is reduced and *counterions* are squeezed out. Q_{cation} can be kept at a certain

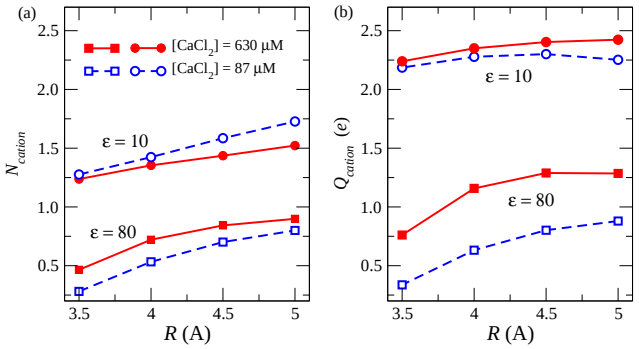

FIG. 6: (color online) (a) Total number of cations N_{cation} and (b) total charge of cations Q_{cation} in the pore as functions of R for $\epsilon = 10$ and 80 at two fixed $CaCl_2$ concentrations. $Q_{cation} = 4$ would be perfect charge neutrality in the pore.

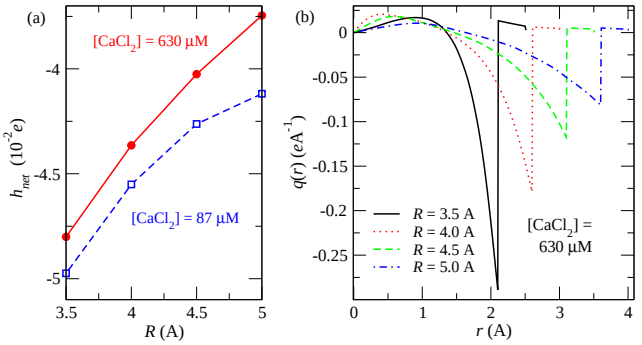

FIG. 7: (color online) (a) Total induced charge h_{net} on the cylindrical wall of the pore as a function of R for $\epsilon = 10$ at two bath $CaCl_2$ concentrations. For $\epsilon = 80$ the induced charge is zero. (b) The radial ionic charge profile in the pore averaged over the axial dimension, $\epsilon = 10$ and $[CaCl_2]$=630 μM.

level (Fig. 6b) while, at the same time, N_{cation} is decreased only if Na^+ is exchanged for Ca^{2+} as shown in Fig. 4. Because of this cation-exchange we obtain better improvement in Ca^{2+} vs. Na^+ selectivity with decreasing R in the case of $\epsilon = 10$ than in the case of $\epsilon = 80$.

One reason for the ion-exchange is the ability of the low dielectric pore to maintain the level of local electroneutrality even if the radius of the pore is decreased. Insight can be gained by considering the average negative induced polarization charges that is determined by the average structure of the ions inside the pore. Figure 7a shows that the average induced charge on the wall of the cylindrical pore becomes more negative as R decreases. Figure 7b shows that near the pore wall the ionic charge is negative, i. e., dominated by the oxygen ions whose fixed number is confined into a smaller space. Fig. 5 indicates that along the z-axis the oxygen ions concentrate mostly near the mouths of the pore cylinder. This distribution of oxygen ions forms a pocket of negative charge around the cations in the pore center (mostly Ca^{2+}).

The increase in negative ionic charge density at the wall results in more negative induced charge on this wall. This average induced charge is small compared to the net ionic charge in the pore, although instantaneously it might be locally large as individual ions move. Induced charge is a separation of charge on the surface and that separation requires energy that is a large component of the free energy of the system. Increasing the cation concentration in the pore reduces both the net ionic charge in the pore and the induced charge on the pore wall (both are negative), and thus reduces the electrostatic energy of the system. This reduction in the electrostatic component of the free energy balances the increasing entropic (excluded volume) component that results from the increase in ionic density. The net result is that the induced charge amplifies the attractive effect of the oxygen ions, but in a complicated, non-additive manner.

In conclusion, the increased Ca^{2+} selectivity of the channel is the result of two mechanisms: (1) decreasing the pore radius R increases ionic density which, in turn, excludes Na^+ from the pore; (2) decreasing the protein dielectric coefficient ϵ increases the number of cations in the pore and produces a constant cationic charge in the pore that does not change as R decreases. Simultaneously decreasing both R and ϵ changes Ca^{2+} selectivity 30-fold, from 1 mM to 30 μM. Any (evolutionary or engineered) changes to the Ca channel protein that specifically modify these two low-resolution parameters can thus tune the ionic selectivity over a fairly wide range.

The authors thank the Ira and Marylou Fulton Supercomputing Center at BYU, the Hungarian National Research Fund (OTKA K63322), NATO Grant PST.CLG.980366, and NIH grant GM067241.

[1] J. Yang, P. T. Ellinor, W. A. Sather, J. F. Zhang, and R. W. Tsien, Nature **366**, 158 (1993).
[2] L. Gao, D. Balshaw, L. Xu, A. Tripathy, C. Xin, and G. Meissner, Biophys. J. **79**, 828 (2000).
[3] M. R. Nelson and W. J. Chazin, BioMetals **11**, 297 (1998).
[4] Y. Yang, D. Henderson, and D. Busath, J. Chem. Phys. **118**, 4213 (2003).
[5] B. Corry, T. Allen, S. Kuyucak, and S.-H. Chung, Biophys. J. **80**, 195 (2001).
[6] B. Corry, T. Vora, and S.-H. Chung, Biochim. Biophys. Acta **1711**, 72 (2000).
[7] W. Nonner, L. Catacuzzeno, and B. Eisenberg, Biophys. J. **79**, 1976 (2000).
[8] D. Boda, D. D. Busath, D. Henderson, and S. Sokołowski, J. Phys. Chem. B **104**, 8903 (2000).
[9] D. Boda, M. Valiskó, B. Eisenberg, W. Nonner, D. Henderson, and D. Gillespie, J. Chem. Phys., **125**, 034901 (2006).
[10] D. Boda, D. Henderson, and D. D. Busath, Mol. Phys. **100**, 2361 (2002).
[11] D. Boda, D. Gillespie, W. Nonner, D. Henderson, and B. Eisenberg, Phys. Rev. E **69**, 046702 (2004).